· Article · Advances in Polar Science
doi: 10.12429/j.advps.2022.0057 June 2023 Vol. 34 No. 2: 105-124

Nitrogen transformation processes in soil along a High Arctic tundra transect

GUO Mengjie[1], WANG Qing[1,2], ZHANG Wanying[1*], JIAO Yi[3], SUN Bowen[1], HOU Lijun[4] & ZHU Renbin[1*]

[1] Institute of Polar Environment & Anhui Province Key Laboratory of Polar Environment and Global Change, School of Earth and Space Sciences, University of Science and Technology of China, Hefei 230026, China;
[2] State Key Laboratory of NBC Protection for Civilian, Beijing 102205, China;
[3] Terrestrial Ecology Section, Department of Biology, Copenhagen University, Copenhagen ØDK-2100, Denmark;
[4] State Key Laboratory of Estuarine and Coastal Research, East China Normal University, Shanghai 200241, China

Received 16 November 2022; accepted 4 April 2023; published online 30 June 2023

Abstract Soil nitrogen (N) transformation processes in the High Arctic tundra are poorly understood even though nitrogen is one of the main limiting nutrients. We analyzed soil samples collected along a High Arctic tundra transect to investigate spatial variability in key nitrogen transformation processes, functional gene abundances, ammonia-oxidizing archaea (AOA) community structures, and key nitrogen transformation regulators. The potential denitrification rates were higher than the nitrification rates in the soil samples, although nitrification may still regulate N_2O emissions from tundra soil. The nutrient (total carbon, total organic carbon, total nitrogen, and NH_4^+-N) contents were important determinants of spatial variability in the potential denitrification rates of soil along the tundra transect. The total sulfur content was the main variable controlling potential nitrification processes, probably in association with sulfate-reducing bacteria. The nitrate content was the main variable affecting potential dissimilatory nitrate reduction to ammonium. AOA and ammonia-oxidizing bacteria *amo*A, *nir*S, and anammox 16S rRNA genes were found in all of the soil samples. AOA play more important roles than ammonia-oxidizing bacteria in soil nitrification. Anammox bacteria may utilize NO_2^- produced through nitrification. Phylogenetic analysis indicated that the AOA *amo*A sequences could be grouped into eight unique operational taxonomic units (OTUs) with a 97% sequence similarity and were affiliated with three group 1.1b *Nitrososphaera* clusters. The results indicated that heterogeneous environmental factors (e.g., the carbon and nitrogen contents of soil) along the High Arctic tundra transect strongly affected the nitrogen transformation rate and relevant functional gene abundances in soil.

Keywords **Arctic tundra soil**, **nitrogen transformation**, **nitrification**, **denitrification**, **functional gene abundance**, **ammonia-oxidizing archaea**

Citation: Guo M J, Wang Q, Zhang W Y, et al. Nitrogen transformation processes in soil along a High Arctic tundra transect. Adv Polar Sci, 2023, 34(2): 105-124, doi: 10.12429/j.advps.2022.0057

1 Introduction

Nitrogen (N) is one of the main limiting nutrients in Arctic tundra soil, and the effectiveness of nitrogen that is present usually depends on nitrogen-compound transformation processes catalyzed by soil microorganisms (Shaver and Chapin, 1980; Nordin et al., 2004; Alves et al., 2013). The main nitrogen transformation processes in natural ecosystems are nitrification, denitrification, anaerobic ammonium oxidation (anammox), dissimilatory nitrate reduction to ammonium (DNRA), and nitrogen fixation,

* Corresponding authors, E-mail: zzwy@ustc.edu.cn (W.Y. Zhang); E-mail: zhurb@ustc.edu.cn (R. B. Zhu)

and these processes are driven by various microbes and form a complex nitrogen cycle (Kuypers et al., 2018). Permafrost soil in the Arctic tundra is a large nitrogen reservoir. It has been conservatively estimated that the top 3 m of soil in the Arctic tundra holds 6.7×10^{10} t of total nitrogen (Harden et al., 2012), which is >500 times more than the amount of nitrogen added to soil as fertilizer each year throughout the world (Bouwman, 2010). When permafrost soil thaws, nitrogen in organic material can be mineralized to NH_4^+, NO_3^-, and NO_2^-, which are involved in nitrification, denitrification, DNRA, and anammox (Voigt et al., 2017a). However, these nitrogen transformations and the functional microbes involved in the Arctic tundra are still poorly understood. It is therefore important to investigate nitrogen transformation processes in the Arctic tundra, particularly because the Arctic is warming faster than the global average (Rysgaard et al., 2004).

It has been found in recent studies that nitrogen transformations in Arctic soil mainly occur in the summer (Zhang et al., 2015; Rasmussen et al., 2021). The degree of nitrogen limitation in Arctic soil is mostly controlled by the nitrification rate (Alves et al., 2013). Ammonia oxidation is the first rate-limiting step in the nitrification process and is performed by phylogenetically and physiologically distinct populations of ammonia-oxidizing archaea (AOA) and ammonia-oxidizing bacteria (AOB) (Belser and Schmidt, 1978; Könneke et al., 2005). The *amo*A gene has been used as a functional marker to analyze AOA and AOB in various environmental media, including sediment (Zheng et al., 2013; Li et al., 2015), oxygenated and suboxygenated ocean water (Baker et al., 2012; Bouskill et al., 2012), plateau permafrost soil (Zhang et al., 2009; Zhao et al., 2017), and subarctic and Arctic soil (Alves et al., 2013; Daebeler et al., 2017). Denitrification is one of the main biological processes causing nitrogen to be lost from the terrestrial environment to the atmosphere and contributes >70% of such nitrogen losses. Denitrification is catalyzed by various metabolic enzymes secreted by denitrifying microorganisms (Dalsgaard et al., 2012; Hou et al., 2013; Baker et al., 2015; Zheng et al., 2015). *nir*S and *nir*K are important functional genes that are involved in denitrification, and *nir*S is more widely distributed than *nir*K in denitrifying microorganisms (Mosier and Francis, 2010; Francis et al., 2013; Smith et al., 2015). *nir*S and *nir*K have been used as gene markers of denitrifying bacteria in glacial foreland soil and polar tundra soil (Heylen et al., 2006; Palmer et al., 2012; Dai et al., 2020). Anammox is a ubiquitous natural process in which bacteria use nitrite as an electron acceptor to oxidize ammonia to nitrogen under anaerobic conditions (Strous et al., 1999; Kuenen, 2008). Anammox has been found to occur in Arctic marine sediment and sea ice and is an important process in the Arctic nitrogen cycle (Rysgaard et al., 2004; Dalsgaard et al., 2005). DNRA is a nitrate reduction pathway that occurs under anaerobic conditions (Fazzolari et al., 1998; Wladyslaw and Robert, 2003). The genes encoding DNRA are found in the genomes of a wide range of soil bacteria (Nelson et al., 2016). DNRA is an important substrate for anammox, and anammox–DNRA coupling can cause more N_2 to be produced than that would happen through anammox or DNRA alone (Kartal et al., 2007; Lam et al., 2009). Nitrogen transformation processes in Arctic soil have been receiving increasing attention in recent years.

Climate warming and permafrost thawing mean nitrogen transformation rates in the Arctic tundra are expected to increase (Rustad et al., 2001; Weintraub and Schimel, 2003; Salmon et al., 2018) because of expected changes in soil moisture contents (MCs), microbial community structures, and litter quality (Rinnan et al., 2008; Rasmussen et al., 2020; Salazar et al., 2020). Evidence has recently been increasing for some Arctic terrestrial ecosystems being globally important sources of N_2O. For example, bare peat and palsa mires have been found to emit large amounts of N_2O, and this could be sustained at low C∶N ratios, the absence of vegetation, high mineral nitrogen availability, and intermediate soil MCs (Repo et al., 2009; Marushchak et al., 2011). N_2O emissions from both bare peatland and permafrost peatland covered in vegetation could increase markedly because of warming and permafrost thawing (Voigt et al., 2017a, 2017b). N_2O is produced through nitrification and denitrification involving anammox and DNRA. It is therefore essential to improve our understanding of nitrogen transformation processes and the functional genes and microbes involved when evaluating N_2O production in Arctic soil and climate feedback processes.

We collected soil samples along a coastal tundra transect in Ny-Ålesund of the High Arctic and analyzed the samples to test the hypothesis that spatial heterogeneity in the physicochemical properties of soil affects nitrogen transformation (nitrification, denitrification, and DNRA) rates, functional gene (AOA and AOB *amo*A, anammox 16S rRNA, and *nir*S) abundances, and AOA community structure coupling with N_2O emissions. The main objectives were (1) to investigate spatial variability in nitrogen transformation rates in soil along the tundra transect, (2) to assess spatial patterns in functional gene abundances and AOA community structures, and (3) to identify the key factors that regulate nitrogen transformation processes in High Arctic tundra soil. The results will help elucidate the effects of spatial heterogeneity in tundra soil on nitrogen transformation processes in the High Arctic and the microorganisms involved.

2 Materials and methods

2.1 Study area

The study was performed at Ny-Ålesund (78°55′N, 11°56′E) on Spitsbergen in the Svalbard Archipelago

(Figure 1). The study area has a High Arctic oceanic climate. The mean annual air temperature at Ny-Ålesund is −5.8 °C, and the mean monthly temperature ranges from −14 °C to 5 °C. The air temperature is >0 °C from June to August, allowing a short growing period for the tundra vegetation. Mean annual precipitation is ~400 mm and gradually decreases to 200–300 mm from the shore to inland (Winther et al., 2002). More than half of the land surface is covered with a seasonally frozen soil layer that starts to melt in early June, and the maximum melted depth of 1.6–2.0 m is reached in early September (Westermann et al., 2010). The tundra from the coastal lowland to the upland areas can be divided into coastal wetland tundra, semi-arid tundra, and upland arid tundra according to altitude. Few plant species are present, and the main species are polar tundra flora such as *Cerastium arcticum*, *Drepanocladus* spp., *Luzula confusa*, *Luzula arctica*, *Salix polaris*, and *Saxifraga oppositifolia*. Moss and lichen cover ~52% and vascular plants cover ~25% of the study area, and ~20% and 3% of the study area is bare soil and rock, respectively (Zhu et al., 2012). Various seabirds and wild animals such as Arctic foxes, geese, and reindeer inhabit the study area (Chen et al., 2014).

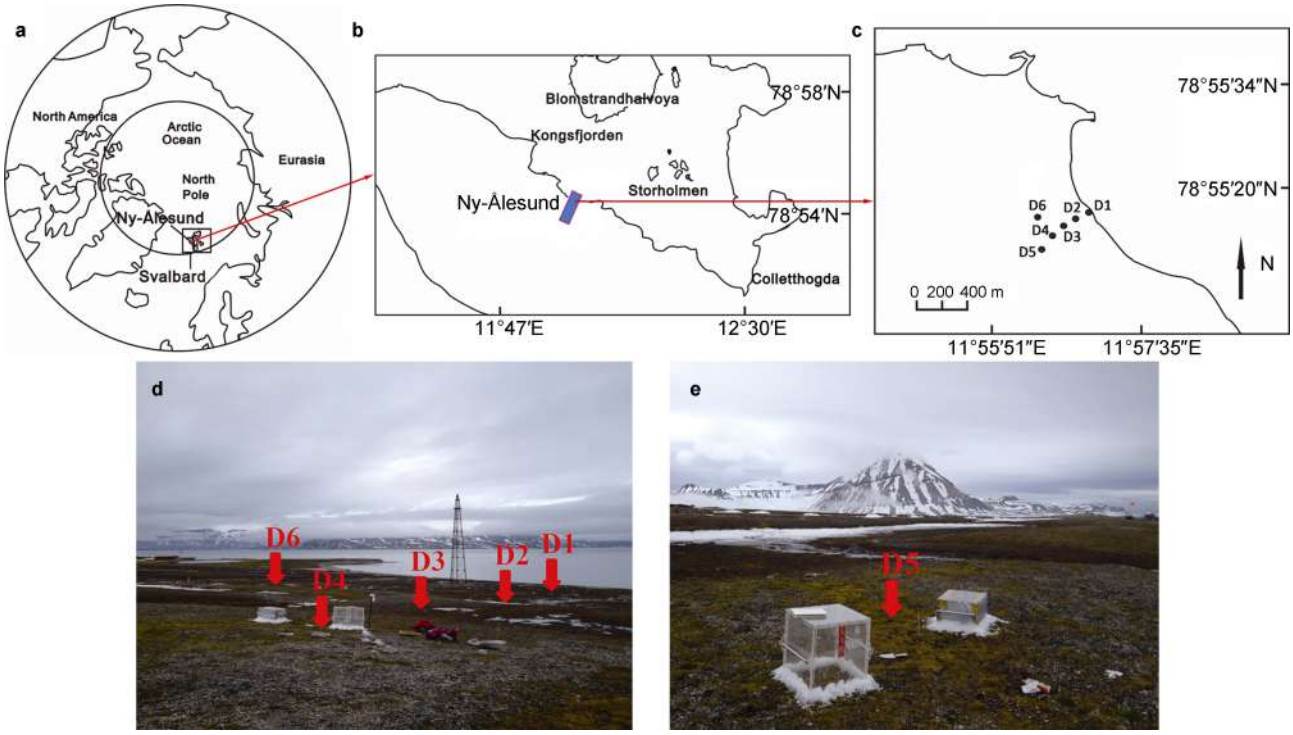

Figure 1 Maps of the study area with the sampling sites marked. **a**, The black square indicates the study area, which is in the High Arctic; **b**, The sampling site locations at Ny-Ålesund in the Svalbard Archipelago; **c**, The locations of the six tundra soil sampling sites (coastal tundra sites D1 and D2 and upland tundra sites D3, D4, D5, and D6) along the tundra transect; **d** and **e**, Photographs of the tundra sites. Note: The maps were adapted with permission from Li et al. (2016).

2.2 Soil collection

Tundra soil samples were collected from six sites along a coastal tundra transect in July 2014. The temperature range during the sampling period was 4.8–7.2 °C. Sampling sites D1 and D2 were close to the coast and had sparse vegetation. The elevation increased through sampling sites D3, D4, D5, and D6, and tundra vegetation coverage increased and the soil became further developed and contained more plant residue material as the altitude increased. At each sampling site, a spoonful of the top 5–10 cm of soil was collected aseptically from each of the four corners of a ~1 m^2 quadrat and the samples were mixed well to give one composite sample. Each sample was immediately divided into two subsamples. One subsample was stored in a sterile plastic container at −80 °C for microbial gene abundance and AOA community structure analyses. The other subsample was stored at the ambient temperature (4 °C) and used to determine the physicochemical properties of the soil and the potential nitrogen transformation (nitrification, denitrification, and DNRA) rates. All analyses were completed within one month of the samples being collected. The N_2O fluxes at the same sites (D1–D6) were determined previously by Li et al. (2016).

2.3 Determining the physicochemical properties of the soil

The soil MC was determined by drying a soil sample at 105 °C to a constant weight. The ammonium nitrogen (NH_4^+-N) and nitrate nitrogen (NO_3^--N) contents were

determined by extracting a sample with 1 mol·L^{-1} KCl and analyzing the extract using a continuous-flow analyzer (Skalar, Breda, Netherlands) (Zhu et al., 2011; Gao et al., 2018). The total organic carbon (TOC) content was determined using the potassium dichromate method. The total carbon (TC), total nitrogen (TN), and total sulfur (TS) contents were determined using a Vario MACRO CNSH analyzer (Elementar Analysensysteme, Langenselbold, Germany). The total phosphorus (TP) content was determined by digesting a sample in a mixture of HNO_3, HCl, HF, and $HClO_4$ in a Teflon tube at 190 °C and then analyzing the digest using a Perkin Elmer 2100DV inductively coupled plasma optical emission spectroscopy system (Perkin Elmer, Waltham, MA, USA).

2.4 Determining the potential nitrogen transformation rate

The soil nitrification rate was determined using the chlorate inhibition method (Kurola et al., 2005; Xia et al., 2007). About 5 g of a fresh soil sample and 20 mL of phosphate-buffered saline induction solution (1 mmol·L^{-1} phosphate buffer, 1 mmol·L^{-1} $(NH_4)_2SO_4$, and 10 mmol·L^{-1} $KClO_3$) were mixed in a 50 mL centrifuge tube and then the tube was incubated in the dark with shaking at 150 rpm for 24 h. A 5 mL aliquot of 2 mol·L^{-1} KCl solution was then added and the mixture was shaken to extract the nitrite. The tube was then centrifuged and the supernatant was transferred to a clean container. A 1 mL aliquot of sulfonamide solution was added to the supernatant and the mixture was shaken for 1 min, then 1 mL of ethylenediamine hydrochloride solution was added and the mixture was shaken for 1 min. The solution was left for 15 min until the color became stable, then the absorbance at a wavelength of 540 nm was measured using a spectrophotometer. A standard curve for $NaNO_2$ standards at concentrations between 0 and 2.5 μmol·L^{-1} was used to calculate the potential nitrification rates in the tundra soil samples.

The soil denitrification rate was determined using a ^{15}N isotope-labeling method (Hou et al., 2015; Cheng et al., 2016). A soil sample and ultrapure water at a volume ratio of 1:7 were mixed to give a uniform slurry, then helium was bubbled through the slurry for >30 min to create an anaerobic environment. The slurry was transferred to an airtight vial and incubated at 5 °C for 48 h with shaking in the dark to eliminate residual nitrate, nitrite, and oxygen. Helium was again bubbled through the slurry for >30 min. The airtight vials containing the soil slurry samples were divided into three groups. To each sample in one group, 200 μL of 50% $ZnCl_2$ was added. To each sample in another group, $^{14}NO_3^-$ was added to give a NO_3^- concentration of 100 mmol·L^{-1}. To each sample in the third group, $^{15}NO_3^-$ was added to give a NO_3^- concentration of 100 mmol·L^{-1}. The samples were incubated at 4 °C for 8 h with shaking in the dark, then the reaction in each sample was inhibited by adding 200 μL of 50% $ZnCl_2$. A strictly anaerobic environment in each sample was maintained throughout the experiment. The $^{14}N^{15}N$ and $^{15}N^{15}N$ abundances in the incubated soil slurry samples were determined by membrane inlet mass spectrometry. The denitrification rate was calculated using a method described in detail in a previous publication (Hou et al., 2015). No anammox activity was detected in the High Arctic tundra soil samples using the slurry incubation method.

The DNRA rate was determined using a method developed by Hou et al. (2012). The DNRA pretreatment and pre-incubation procedures were the same as the denitrification pretreatment and pre-incubation procedures. After nitrogen was eliminated by bubbling helium through the slurry to ensure that the slurry was anoxic, 0.1 mL of a solution containing $^{15}NO_3^-$ at a concentration of 12.5 mmol·L^{-1} was added through the septum of the vial to give a final $^{15}NO_3^-$ concentration of ~100 μmol·L^{-1} (final ^{15}N concentration as a percentage of the TN concentration 90%–99%). The vials were divided into two groups. To each vial in one group, 200 μL of 50% $ZnCl_2$ was added immediately to inhibit nitrogen transformation reactions. The vials in another group were then incubated at 4 °C for 8 h and then 200 μL of 50% $ZnCl_2$ was added to each vial in the group to stop any further reactions. N_2 generated through denitrification and anammox was eliminated by bubbling helium through the slurry in each vial, then the vials were refilled. $^{15}NH_4^+$ produced through DNRA was oxidized to nitrogen ($^{14}N^{15}N$ and $^{15}N^{15}N$) by adding 200 μL of iodine hypobromite solution. The $^{14}N^{15}N$ and $^{15}N^{15}N$ abundances in each incubated slurry sample was determined by membrane inlet mass spectrometry. The R_{DNRA} value was calculated using the equation

$$R_{DNRA} = \frac{\left[{}^{15}NH_4^+\right]_1 - \left[{}^{15}NH_4^+\right]_2}{W \cdot T},$$

where $[\,{}^{15}NH_4^+\,]_1$ is the $^{15}NH_4^+$ concentration at the beginning of the slurry incubation, $[\,{}^{15}NH_4^+\,]_2$ is the $^{15}NH_4^+$ concentration after 8 h of incubation, W is the sample mass, and T is the incubation time.

2.5 DNA extraction, gene amplification, sequencing, and phylogenetic analysis

Total genomic DNA was extracted from 0.25 g of each mixed soil sample using a PowerSoil DNA isolation kit (Mo Bio, Carlsbad, CA, USA) following the protocol supplied by the supplier. The extracted DNA was eluted with 50 μL of elution buffer, quantified using a Nanodrop-2000 spectrophotometer (Thermo Fisher Scientific, Waltham, MA, USA), and stored at −20 °C. The *amo*A gene fragments (635 bp) of AOA were amplified using the primers arch-amoAF (5'-STAATGGTCTGGCTTAGACG-3') and arch-amoAR (5'-GCGGCCATCCATCTGTATGT-3') (Francis et al., 2005). Polymerase chain reaction (PCR) amplification using a total volume of 50 μL was performed using Taq PCR

Master Mix (Sangon Biotech, Shanghai, China). The PCR amplification procedure was 95 °C at 5 min; 30 cycles of 94 °C for 30 s, 56 °C for 45 s, 72 °C for 1 min; and a final 5 min extension cycle at 72 °C (Zheng et al., 2014).

The amplification products were purified, cloned, and sequenced (Sangon Biotech, Shanghai, China) as described in previous publications (Zheng et al., 2014; Wang et al., 2019). The sequences were edited using DNAStar (DNASTAR, Madison, WI, USA). The sequences were aligned using the multiple sequence comparison by log-expectation method (Edgar, 2004) using the unweighted pair group method with arithmetic mean clustering method in ClusalX (version 2.1) software with default parameters. Sequences with 97% identities were classed as operational taxonomic units (OTUs) using the furthest neighbor approach using Mothur software (http://www.mothur.org/wiki/Main_Page). The rarefaction curve (Supplementary Figure S1) indicated that these clones represented most of the types of archaea in the library. The closest reference sequences were identified in the NCBI database (http://www.ncbi.nlm.nih.gov/BLAST/) using the BLASTn tool (Madden, 2002), and a phylogenetic tree was constructed using the adjacency method using Molecular Evolutionary Genetics Analysis version 5.03 software (https://www.megasoftware.net/). The relative confidence for the tree topology was determined by performing 1000 bootstraps to test the topological stability of the phylogenetic tree (Tamura et al., 2007). The sequences reported here were deposited in GenBank under accession numbers OP822030–OP822037.

2.6 Quantitative real-time PCR

The AOA and AOB *amo*A, *nir*S and anammox 16S rRNA gene abundances in the soil samples were determined by quantitative real-time PCR using an Applied Biosystems ABI 7500 sequence detection system (Thermo Fisher Scientific, Waltham, MA, USA) (Hou et al., 2013; Zheng et al., 2014). Triplicate analyses of each sample were performed, and the specificity of the quantitative real-time PCR amplification system was determined using melting curves (Supplementary Figures S2–S5) and agarose gel electrophoresis. A standard curve was constructed by continuous quantitative dilution of the plasmid to allow the gene abundances to be calculated. Plasmid DNA concentrations were determined using a Nanodrop-2000 spectrophotometer (Thermo Fisher Scientific, Waltham, MA, USA). The quantitative real-time PCR assay was found to give consistent results because there was a strong inverse linear relationship between the threshold cycle and log value of the gene copy number for each primer set (R^2 = 0.997, 0.996, 0.996, and 0.998 for AOA *amo*A, AOB *amo*A, *nir*S, and anammox 16S rRNA, respectively). The AOA *amo*A, AOB *amo*A, *nir*S, and anammox 16S rRNA amplification efficiencies were 92.4%, 95.0%, 90.5%, and 91.3%, respectively. In each experiment, negative controls were analyzed to allow any possible contamination or carryover to be detected and excluded. Specific primer information is shown in Supplementary Table S1.

2.7 Statistical analysis

The Shannon index, Simpson index, and richness estimator Chao1 for each constructed gene library were calculated using Mothur (version 1.23.0) software. The clone library coverage was estimated by dividing the number of observed OTUs by the percentage contribution of Chao1. The nitrogen transformation rates, microbial gene abundances, and significances of the differences for soil at the tundra sites were determined using Origin 2021b software (OriginLab, Northampton, MA, USA). Correlations between the physicochemical properties, nitrogen transformation rates, functional gene abundances, and N_2O fluxes for soil at the tundra sites were determined using Excel software (Microsoft, Redmond, WA, USA) and SPSS statistics 17 software (IBM, Armonk, NY, USA), and Pearson correlation analyses were performed to identify correlations. Correlation plots and confidence intervals were produced using Origin 2021b software.

3 Results

3.1 Physicochemical properties of the High Arctic tundra soil samples

As shown in Table 1, the tundra soil samples from the coastal sites D1 and D2 were very waterlogged and anoxic and had low NH_4^+-N, NO_3^--N, TC, TN, and TOC contents because they had sandy textures. The MCs of the samples from sites D3, D4, D5, and D6 decreased as the altitude increased, as shown in Figure 1c and 1d, but the differences in the MCs for these four sites were small. The TC, TN, TOC, and TP contents were much higher for the samples from sites D3, D4, D5, and D6 than the samples from sites D1 and D2 because of the well-developed vegetation and soil at sites D3–D6. The NH_4^+-N and NO_3^--N contents were one–two orders of magnitude higher for the samples from sites D3, D4, D5, and D6 than the samples from sites D1 and D2. The NH_4^+-N, NO_3^--N, TC, TN, and TOC contents and C∶N ratio were lower for the sample from site D4 than the samples from sites D3, D5, and D6, possibly because the vegetation was more sparse at site D4 than sites D3, D5, and D6. The TS contents of the samples from all of the sites were 0.13%–0.49%, and the differences were smaller than the differences in the other environmental variables. The C∶N ratios varied widely, from 12.8 to 21.9. Overall, the NH_4^+-N, NO_3^--N, TC, TN, TOC, and TP contents were higher at the upland tundra sites than at the waterlogged coastal tundra sites.

3.2 Nitrogen transformation rates for soil along the tundra transect

The potential nitrification rates for the samples from

Table 1 Physicochemical properties of the tundra soil samples

Sampling No.	Altitude/m	MC/%	NH_4^+-N /(mg·kg^{-1})	NO_3^--N (mg·kg^{-1})	TN/%	TC/%	TOC/%	TS/%	TP/%	C:N
D1	0	Waterlogged	0.28	0.11	0.39	5.26	2.65	0.13	0.96	13.5
D2	4	Waterlogged	0.98	0.27	0.34	7.55	2.87	0.15	1.07	21.9
D3	8	71.4	18.74	0.81	1.86	28.47	14.63	0.35	2.35	15.3
D4	10	67.1	10.23	0.70	1.18	15.13	8.14	0.15	2.49	12.8
D5	15	50.3	19.16	1.16	1.72	26.57	12.33	0.16	2.44	15.5
D6	9	74.1	12.60	1.19	1.76	24.03	12.46	0.49	-	13.6

along the tundra transect were 0.65–2.18 (nmol N)·g^{-1}·h^{-1}, and the highest (2.18±0.40 (nmol N) ·g^{-1}·h^{-1}, which was significantly higher (p<0.05) than the potential nitrification rates found at the other sites) was found for site D6, at which the highest NO_3^--N content was also found. Higher potential denitrification rates were found for sites D3 (5.86±0.52 (nmol N)·g^{-1}·h^{-1}), D5 (3.73± 0.46 (nmol N)·g^{-1}·h^{-1}), and D6 (3.74±0.16 (nmol N)·g^{-1}·h^{-1}) than for sites D1, D2, and D4 because the NH_4^+, NO_3^-, TC, TN, and TOC contents were higher for sites D3, D5, and D6 than sites D1, D2, and D4 (Figure 2 and Table 1). The soil at site D1 had an extremely low potential denitrification rate because it had the lowest MC, NH_4^+, NO_3^-, TN, TOC, TP, and TS contents. The potential DNRA rate increased as the altitude increased, and the highest potential DNRA rate (0.63± 0.04 (nmol·N)·g^{-1}·h^{-1}) was found for site D5. The potential DNRA rates were significantly lower (p<0.05) for sites D1 and D2 than sites D4, D5, and D6. The mean potential denitrification rate for the transect was 3.03± 1.79 (nmol N) ·g^{-1}·h^{-1}, which was significantly higher (paired t-test, p<0.05) than the mean potential nitrification rate (1.16±0.05 (nmol N)·g^{-1}·h^{-1}) and one order of magnitude higher than the mean potential DNRA rate (0.33±0.17 (nmol N)·g^{-1}·h^{-1}). No anammox activity was detected at any of the sites even though anammox 16S rRNA genes were found in the soil samples (see Section 2.4).

Pearson correlation analysis (Figure 3 and Supplementary Table S2) indicated that the potential denitrification rate significantly positively correlated with the TC content (r=0.915, p=0.01), TOC content (r=0.915, p=0.01), TN content (r=0.874, p=0.02), and NH_4^+-N content (r=0.881, p=0.02), indicating that well-developed soil and sufficient nutrients promoted denitrification activity. The potential nitrification and DNRA rates only significantly positively correlated with the TS content (r=0.847, p=0.03) and nitrate content (r=0.824, p=0.04), respectively.

3.3 Functional gene abundances related to nitrogen transformations in the tundra transect soil samples

The functional genes AOA *amo*A and AOB *amo*A (for

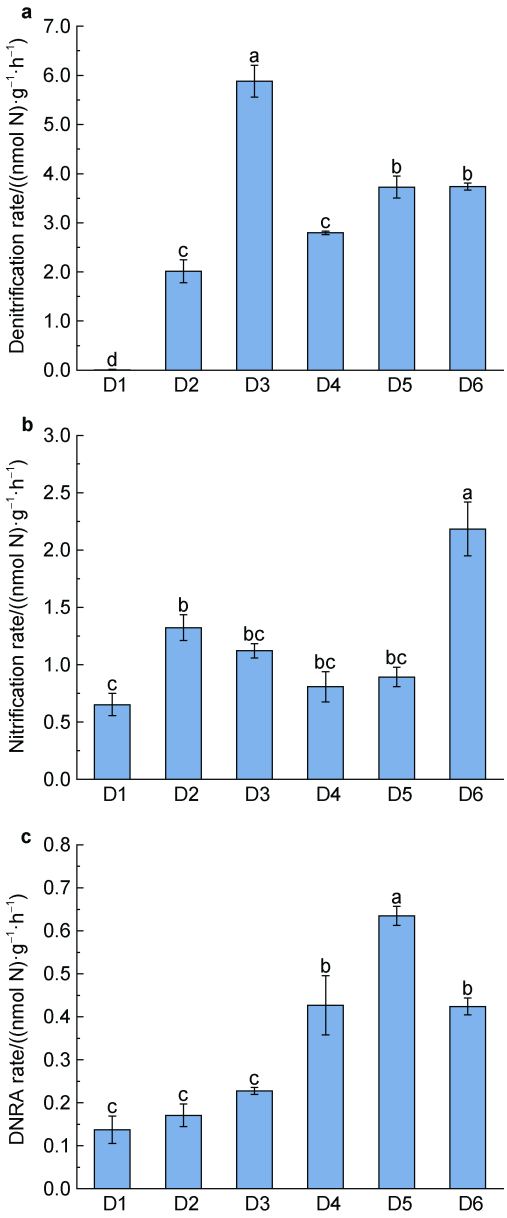

Figure 2 Potential denitrification (**a**), nitrification (**b**), and dissimilatory nitrate (**c**) reduction to ammonium (DNRA) rates for the soil samples from sites D1–D6 along the High Arctic tundra transect. Each error bar indicates the standard deviation (n=3). Bars labeled with the same letter were not significantly different (p<0.05).

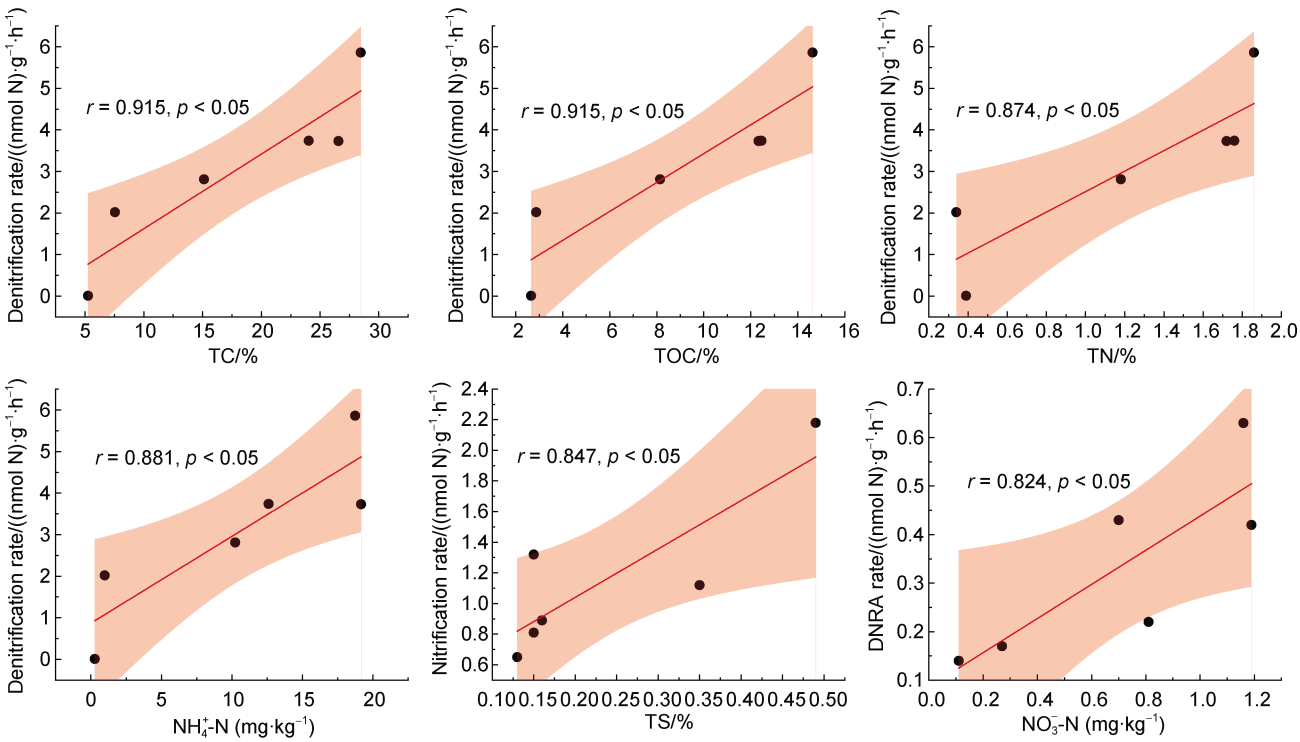

Figure 3 Relationships between the potential denitrification, nitrification, and DNRA rates and environmental variables in the High Arctic tundra transect soil samples. Each shaded area indicates the 95% confidence level range.

ammonia oxidation), *nir*S (for denitrification), and anammox 16S rRNA (for anaerobic ammonia oxidization) were detected in the soil samples from all of the sites (Figure 4). The AOA *amo*A gene abundances (mean $(9.09\pm0.91)\times10^6$ copies in 1 g soil sample) were significantly higher (paired *t*-test, $p<0.05$) than the AOB *amo*A gene abundances (mean $(3.20\pm1.31)\times10^6$ copies in 1 g soil sample). The highest AOA *amo*A gene abundance (mean 3.77×10^6 copies in 1 g soil sample) was found for site D6 and the lowest (1.52×10^6 copies in 1 g soil sample) was found for site D4. The AOA *amo*A gene abundances were significantly higher ($p<0.05$) for sites D1, D5, and D6 than sites D2, D3, and D4. However, the AOB *amo*A gene abundances were significantly higher ($p<0.05$) for sites D1–D3 than sites D4–D6, and the lowest abundance was found for site D4 (6.46×10^4 copies in 1 g soil sample) and the highest abundances were found for sites D1 and D3 (4.41×10^4 copies in 1 g soil sample). The mean *nir*S gene abundance was $(9.07\pm1.95)\times10^6$ copies in 1 g soil sample, and the lowest abundance was found for site D3 (6.32×10^6 copies in 1 g soil sample) and the highest abundance was found for site D5 (1.24×10^7 copies in 1 g soil sample). The *nir*S gene abundances were significantly higher ($p<0.05$) for sites D1, D5, and D6 than sites D2, D3, and D4. The anammox 16S rRNA gene abundances varied strongly along the tundra transect and the mean was $(8.48\pm8.16)\times10^7$ copies in 1 g soil sample. The anammox 16S rRNA gene abundances for the different sites were significantly different ($p<0.05$), and the highest was found for site D6 (2.57×10^8 copies in 1 g soil sample) and the lowest was found for site D1 (1.39×10^6 copies in 1 g soil sample).

No significant correlations ($p>0.05$) were found between the abundances of the functional genes and environmental factors (Supplementary Table S3), possibly because of the relatively high variability in the functional gene abundances and environmental factors along the tundra transect. The AOA and AOB *amo*A gene abundances did not significantly correlate ($p>0.05$) with the potential nitrification and other nitrogen conversion rates (Supplementary Table S4). The *nir*S gene abundance significantly positively correlated with the potential DNRA rate ($r=0.812$, $p<0.05$) but did not correlate with the potential denitrification rates (Figure 5b). The anammox 16S rRNA gene abundance significantly positively correlated with the potential nitrification rate ($r=0.893$, $p=0.05$).

The N_2O emission rate significantly positively correlated with the potential nitrification rate ($r=0.93$, $p<0.05$) but did not correlate with the potential denitrification rate ($r=0.504$, $p=0.387$) (Figures 5c and 5d), suggesting that N_2O emissions were mainly driven by nitrification mediated by nitrifiers (AOA and AOB). The AOA community structure was therefore analyzed (see Section 2.5) because AOA *amo*A genes were significantly more abundant than AOB *amo*A genes (Figure 4).

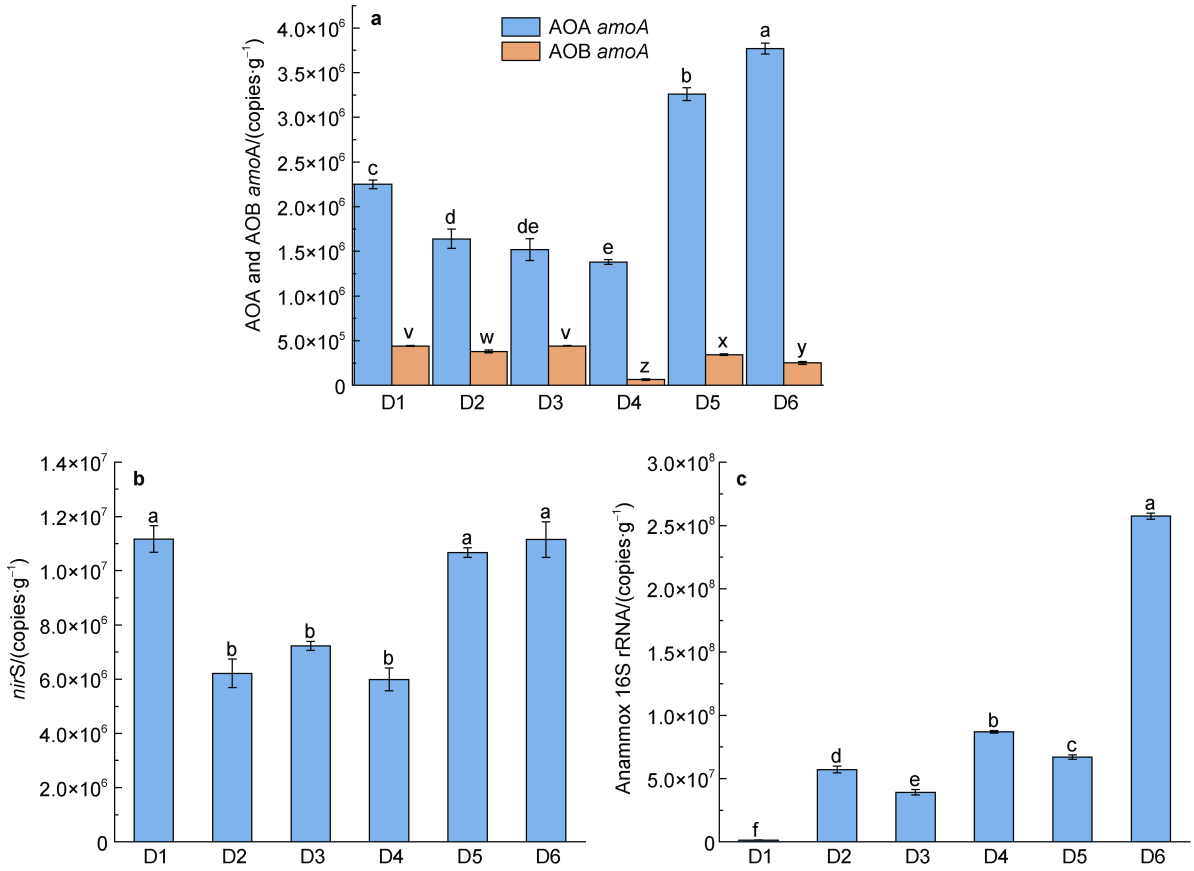

Figure 4 **a**, Ammonia-oxidizing archaea (AOA) and ammonia-oxidizing bacteria (AOB) *amo*A; **b**, *nir*S; **c**, Anammox 16S rRNA gene abundances in the High Arctic tundra transect soil samples. Each error bar indicates the standard deviation (n=3).

3.4 AOA community structures in the tundra transect soil samples

A total of 307 valid AOA *amo*A gene sequences were obtained through clone library sequencing of the soil samples from the six tundra transect sites. Two–eight AOA OTUs were identified (defined as <3% nucleotide divergence) for each site. As shown in Table 2, the AOA *amo*A genes were more diverse in the soil samples from the coastal sites D1 and D2 than the soil samples from the upland sites D3–D6 according to the Shannon diversity index and reciprocal of Simpson's diversity index. Phylogenetic analysis indicated that the AOA *amo*A sequences could be divided into eight different OTUs with 97% sequence similarities to allow comparisons and classification to be performed to represent 100% of the AOA *amo*A OTUs that were identified. These sequences were affiliated with three 1.1b *Nitrososphaera* clusters (Figure 6). Cluster I contained four OTUs and 192 clones, with 26.0% of the AOA *amo*A sequences from the coastal tundra soil samples and 74.0% from the upland tundra soil samples. Cluster II contained only two OTUs and 55 clones, with 78.2% from the coastal tundra soil samples and 21.8% from the upland tundra soil samples. Cluster III contained two OTUs and 53 clones, with 90.6% from the upland tundra soil samples and only 9.4% from the coastal tundra soil samples. The AOA phylotypes for the coastal and upland tundra soil samples could be divided into three clusters, most of which were related to cluster I. Almost all of the AOA phylotypes for the coastal tundra soil samples were related to *Nitrososphaera* clusters I and II, but the AOA phylotypes for the upland tundra soil samples were in clusters I and III.

4 Discussion

4.1 Effects of environmental heterogeneity on nitrogen transformation rates in soil

The physicochemical characteristics, MCs, temperatures, and plant communities are different at different locations in the High Arctic tundra. These result in strong environmental heterogeneity over short distances and therefore strong variability in nitrogen transformation processes in soil (Nadelhoffer et al., 1992; Walker et al., 2008). In our study area, the strong variations in the nitrogen transformation rates were probably caused by variations in the physicochemical properties of the soil, microbe populations, and vegetation along the transect (Figure 2 and Table 1). The MC and organic matter content

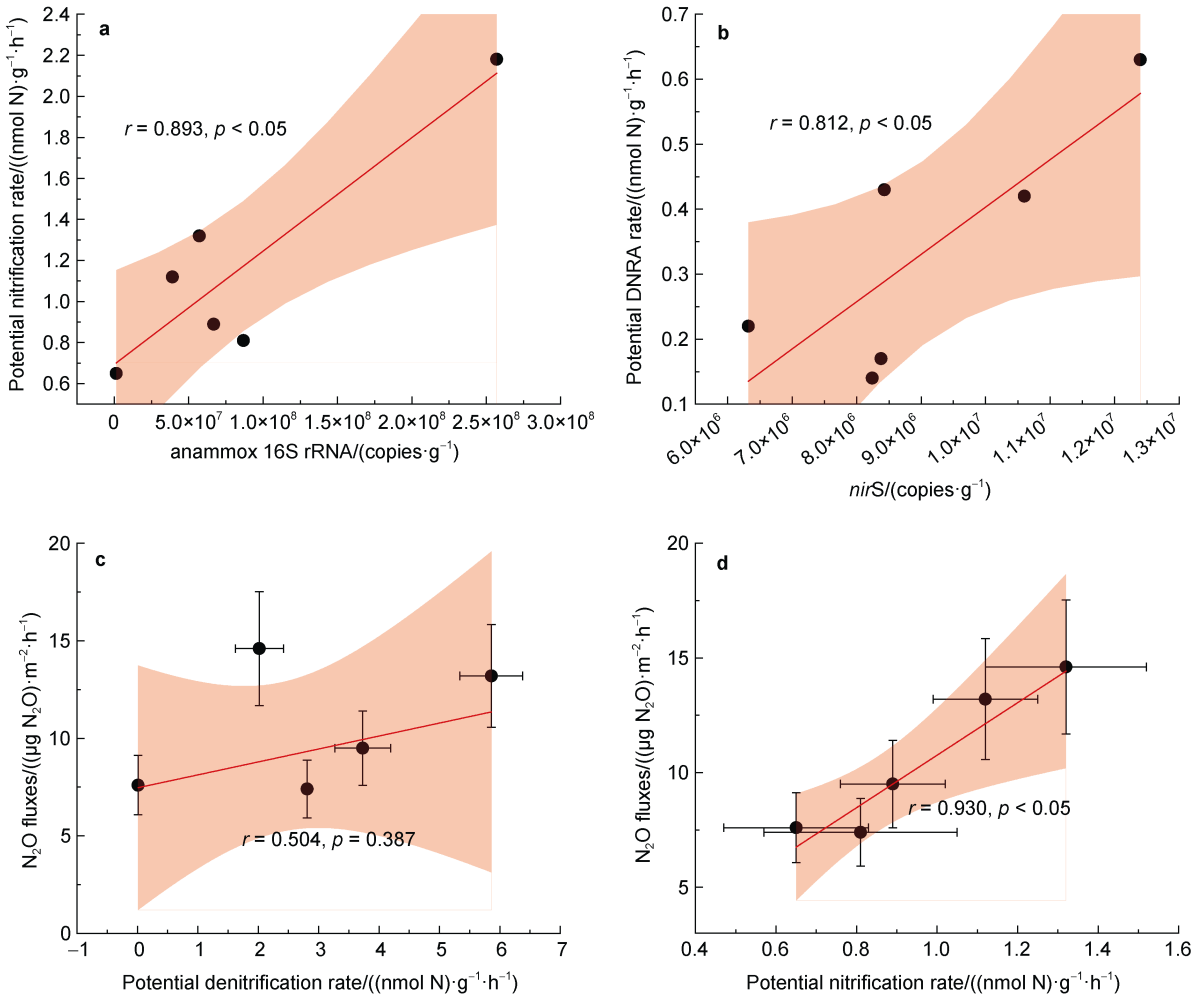

Figure 5 Relationships between the potential nitrification rate and anammox 16S rRNA gene abundance (**a**) and the potential dissimilatory nitrate reduction to ammonium (DNRA) rate and *nir*S gene abundance (**b**) in the high Arctic tundra soil samples. Lines fitted to the N_2O fluxes from the sampling sites plotted against the potential denitrification rate (**c**) and the potential nitrification rate (**d**). Each error bar indicates the standard deviation (n=3). The N_2O flux data were taken from a publication by Li et al. (2016) with permission to allow correlations between the fluxes and potential nitrification and denitrification rates to be identified.

Table 2 Clone library diversity characteristics for the AOA *amo*A genes in the tundra transect soil samples

Sampling No.	No. of clones	OTUs [a]	Chao1[b]	Shannon[c]	1/Simpson[d]	Coverage[e]
D1	51	8	11.5	0.91	1.65	70.7%
D2	50	5	5	0.75	1.54	100%
D3	51	2	2	0.09	1.17	100%
D4	51	3	3	0.52	1.42	100%
D5	52	2	2	0.09	1.04	100%
D6	52	4	5	0.51	1.33	80%

Notes: a, OTUs were defined at 3% nucleotide acid divergence;
b, Nonparametric statistical predictions of the total richnesses of the OTUs were based on the singleton and double distributions;
c, Shannon diversity index. A higher number indicates more diversity;
d, Reciprocal of Simpson's diversity index. A higher number indicates more diversity;
e, Percentage coverage: the percentage of the observed number of OTUs divided by the estimates Chao1.

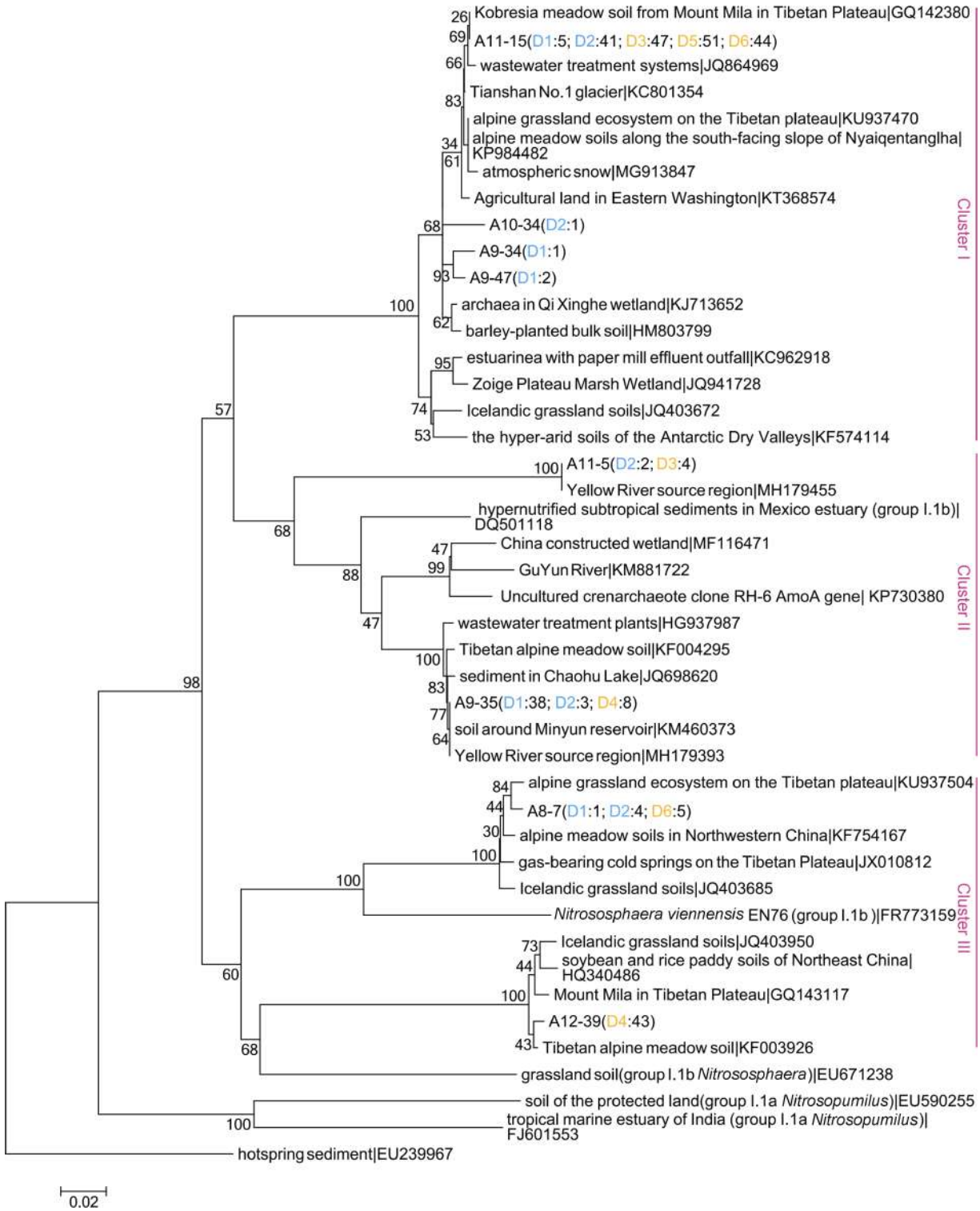

Figure 6 Neighbor-joining phylogenetic tree of for the AOA *amo*A genes. OTUs were defined as 97% similarity. The numbers in parentheses after each OTU value indicate the number of sequences recovered from the samples from the relevant sampling sites.

of Arctic soil are generally considered to be key determinants of denitrification activity (Walker et al., 2008; Banerjee and Siciliano, 2012a; Canion et al., 2014). Carbon is the main element required by heterotrophic anaerobic microorganisms for denitrification, and biodegradable organic matter is the best electron donor for denitrification. A high organic carbon content will therefore increase the microbial denitrification rate (Rezvani et al., 2019; Rajta et al., 2020; Gao et al., 2022). The potential denitrification rates and the NH_4^+-N , TC, TN, and TOC contents

significantly positively correlated (p<0.05), indicating that the organic matter and nitrogen contents were important determinants of spatial variability in the potential denitrification rates in the tundra transect soil samples (Figure 3 and Supplementary Table S2). Denitrification and DNRA are competitive nitrate reduction pathways (Wladyslaw and Robert, 2003; Giblin et al., 2013; Lu et al., 2013). The balance between denitrification and DNRA is critical because denitrification causes bioavailable nitrogen to be lost (Roberts et al., 2022). The significant correlation between the potential DNRA rate and NO_3^--N content indicated that the nitrate content was the main environmental variable that affected DNRA in soil (Figure 3).

The potential nitrification rate significantly positively correlated with the sulfur content (Figure 3) but weakly positively correlated with the NH_4^+-N, NO_3^--N, TC, TN, and TOC contents (Supplementary Table S2), indicating that the TS content was the main environmental variable controlling nitrification in soil and that nitrification could be related to sulfate-reducing bacteria. Some sulfate-reducing bacteria can use elemental sulfur and nitrate as electron acceptors and reduce them to sulfide and ammonium, respectively (Fauque et al., 1991; Madigan and Martinko, 2006). We speculated that sulfate-reducing bacteria in tundra soils could reduce SO_4^{2-} and NO_3^- to sulfide and NH_4^+ to form a coupled nitrification cycle.

The denitrification rate is generally affected by the abundance of denitrifying bacteria encoded by the *nir*S gene (Mosier and Francis, 2010; Gao et al., 2016), and the nitrification rate is closely related to the AOA and AOB *amo*A gene abundances (Wang et al., 2019; Dai et al., 2020). However, no significant correlations were found between the potential denitrification rate and *nir*S gene abundance or the potential nitrification rate and AOA or AOB *amo*A gene abundances (Supplementary Table S4). This was probably because the control of denitrification and nitrification exerted by soil microorganisms is masked in nutrient-poor tundra soil because of serious nutrient constraints, meaning the physicochemical properties of the soil rather than functional genes are the main factors controlling the ammonia oxidation and denitrification potentials in harsh High Arctic environments (Banerjee et al., 2011; Banerjee and Siciliano, 2012a). Our results indicated that environmental heterogeneity strongly affects nitrogen transformation rates in soil even along a short tundra transect.

4.2 Effects of environmental heterogeneity on functional gene abundances in soil

It has previously been found that AOA *amo*A genes are usually more abundant than AOB *amo*A genes in nutrient-poor terrestrial and marine environments (Leininger et al., 2006; Wuchter et al., 2006; Lam et al., 2007; Schleper, 2010; Yao et al., 2011; Cao et al., 2013). In this study, AOA *amo*A genes were more abundant than AOB *amo*A genes in all of the soil samples (Figure 4), which was consistent with the results of the previous studies mentioned above. AOA and AOB generally inhabit different soil niches determined by the NH_4^+ content and availability (Verhamme et al., 2011; Wessén et al., 2011). AOA may be better adapted than AOB to low NH_4^+ content oligotrophic environments in maritime Antarctic soil (Wang et al., 2019). In a batch culture experiment, AOA were more abundant in a poor nutrient system with a low NH_4^+ content and AOB were more abundant in a medium/high nutrient system with a high NH_4^+ content (French et al., 2021). Roy et al. (2020) found in a laboratory study that a lower NH_4^+ content was favorable to AOA rather than AOB and that AOA *amo*A genes were more abundant than AOB *amo*A genes. The NH_4^+-N and TN contents of the High Arctic tundra soil samples were generally low, indicating that NH_4^+-N and TN could not be continually replenished (Table 1). Microorganisms in tundra soil will compete strongly for nutrients, and NH_4^+ is the only source of energy and nitrogen available to AOA and AOB (Liu et al., 2021). The higher AOA *amo*A abundances than AOB abundances may therefore be related to the low nitrogen contents of the tundra transect soil samples.

No significant correlations were found between the *nir*S gene abundance and environmental variables (Supplementary Table S3). However, the *nir*S gene abundance significantly positively correlated with the potential DNRA rate (Figure 5 and Supplementary Table S4), suggesting that there may be a competitive balance between microbes related to DNRA and denitrifying bacteria in nutrient-poor tundra soil and that various environmental variables affect microbe abundances (Fazzolari et al., 1998; Wladyslaw and Robert, 2003; Roberts et al., 2022). Anammox bacteria are strictly thermophilic and are found in hypoxic or anoxic environments (Ward, 2003; Galán et al., 2012; Canion et al., 2014). Our results indicated that anammox 16S rRNA genes are widespread in High Arctic tundra soil even though anammox activity was not detected (Figure 4). The anammox 16S rRNA gene abundance significantly positively correlated with the potential nitrification rate (Figure 5 and Supplementary Table S4), suggesting that anammox bacteria could utilize NO_2^- produced through nitrification (Spott et al., 2011; Phillips et al., 2016; Qin et al., 2017). Vipindas et al. (2020) found that anammox reactions widely occurred in oxygen-containing surface sediment in an Arctic fjord. The NO_3^- contents were lower than the NH_4^+ contents of our tundra soils (Table 2), but anammox 16S rRNA genes were one–two orders of magnitude more abundant than AOA and AOB *amo*A genes (Figure 4), indicating that anammox may occur, i.e., NH_4^+ may be oxidized by AOA and AOB to NO_2^-, which is then consumed through anammox with the remaining NH_4^+ (Qin et al., 2017).

4.3 Effects of environmental heterogeneity on the AOA community in tundra soil

Archaea can grow and reproduce even in harsh environments and are widely distributed in Arctic ecosystems (Francis et al., 2005). Archaea 16S rRNA genes can be as abundant as 10^{10} copies in 1 g soil sample in Arctic soil (Banerjee et al., 2011), and AOA can account for 10% of the total prokaryotic community in soil (Hatzenpichler, 2012; Zhalnina et al., 2012). In previous studies, 10^5–10^7 copies were found in 1 g soil sample AOA gene when Arctic soil samples were analyzed (Banerjee and Siciliano, 2012b; Alves et al., 2013) and fewer AOB gene copies were found (Leininger et al., 2006). These results agreed with our results. AOA have lower levels of microbial diversity in the most extreme environments than in benign environments (Cowan et al., 2015). Only two–eight AOA OTUs were identified in our tundra soil samples, and the AOA *amo*A genes (Table 2) were less diverse than AOA *amo*A genes found in other environments (Zheng et al., 2013; Li et al., 2015; Zhao et al., 2017). It is generally believed that the MC, pH, and TC content of soil are key factors driving archaea community structures and AOA in Arctic tundra soil (Banerjee et al., 2016). The more diverse AOA *amo*A genes in the coastal tundra soil from sites D1 and D2 than in the soil from sites D3–D6 may therefore have been related to the higher MCs and C∶N ratios for the soil from sites D1 and D2 than for the soil from sites D3–D6 (Table 1).

The AOA for all of the soil samples were in the group l.1b *Nitrososphaera* cluster (Figure 6), which contains AOA that are mainly found in low-salt environments such as soil, intertidal zones, and estuaries (Hatzenpichler, 2012). The AOA phylotypes in most of the High Arctic tundra soil samples were related to cluster I. The OTUs detected in cluster I most closely matched OTUs found in alpine meadow soil (GQ142380, KU937470, KP984482, and JQ403672), glacial soil (KC801354), hyper-arid soil from the Antarctic Dry Valleys (KF574114), wetland soil (KJ713652 and JQ941728), agricultural soil (KT368574 and HM803799), and soil affected by wastewater treatment plants (JQ864969 and KC962918). Cluster II was more prevalent in the coastal tundra soil samples, and the sequences were affiliated with sequences previously found in aquatic environments such as the Yellow River (MH179455 and MH179393), Chaohu Lake sediment (Q698620), and soil from around Minyun Reservoir (KM460373). Cluster III was most prevalent in the upland tundra soil samples, and the sequences were affiliated with the sequences previous found in alpine meadow soil (KU937504, KF754167, JQ403685, JQ403950, and KF003926) and soil from other cold environments (FR773159 and GQ143117). Our results indicated that environmental heterogeneity could have affected the AOA community composition in the soil along the tundra transect.

4.4 Contribution of nitrification to N_2O emissions from High Arctic tundra soil

Regression analysis indicated that the N_2O flux was directly proportional to the potential nitrification rate (p<0.05) along the tundra transect but that the N_2O flux did not significantly correlate with the potential denitrification rate (Figures 5c and 5d). Similar results were found for the N-limited Arctic Truelove Lowland, where most N_2O emitted from soil was found to be related to nitrification rather than denitrification (Ma, 2007; Siciliano et al., 2009). Nitrification has been found to consume about half of the mineralized nitrogen in some Arctic soils and to contribute more than other processes to N_2O emissions (Giblin et al., 1991; Ma, 2007; Siciliano et al., 2009). DNRA is an important substrate for ammonia oxidation (Kartal et al., 2007; Lam et al., 2009), which increases the NH_4^+-N content of soil (Table 1). The much higher NH_4^+-N contents than NO_3^--N contents and the significant correlation between the N_2O flux and nitrification rate indicated that nitrification was the main contributor to N_2O emissions from soil along our High Arctic tundra transect.

Ammonia oxidation by AOA and AOB is the rate-limiting step for nitrification and strongly affects N_2O emissions from Arctic soil (Könneke et al., 2005). AOB can couple nitrification and nitrifier denitrification to produce N_2O, which mainly occurs in low-oxygen environments (Cantera and Stein, 2007; Caranto and Lancaster, 2017). AOA can produce N_2O through the reaction between the intermediate NO and hydroxylamine (Kozlowski et al., 2014) and can oxidize ammonia at low oxygen concentrations (Liu et al., 2021). AOA are the main contributors to N_2O emissions from the ocean (Santoro et al., 2011), and AOA enrichment experiments have indicated that mixed metabolic pathways produce N_2O in soil (Jung et al., 2014). AOA has been found to be an important driver of ammonia oxidation and to be involved in N_2O emissions from Arctic tundra soil (Ma, 2007; Siciliano et al., 2009; Banerjee and Siciliano, 2012b). AOA *amo*A genes were markedly more abundant than AOB *amo*A genes in our samples (Figure 4), indicating that N_2O production in the High Arctic tundra soil was mainly caused by AOA.

5 Conclusions

The potential denitrification rate was higher than the potential nitrification rate along the High Arctic tundra transect when the temperature was <4 °C and the NH_4^+-N, TC, TN, and TOC contents were the key factors determining the denitrification activity. Potential nitrification was primarily controlled by the TS content and potential DNRA was mainly controlled by the nitrate content. The N-transformation functional genes AOA *amo*A, AOB *amo*A, *nir*S, and anammox 16S rRNA were found

widely in the soil samples. AOA in the soil samples were in the group 1.1b *Nitrososphaera* cluster, and the oligotrophic natures of AOA mean they play important roles driving ammonia oxidation in nutrient-limited tundra soil. Anammox bacteria in soil could use NO_2^- produced during nitrification. Overall, environmental heterogeneity along the tundra transect was found to determine the soil nitrogen transformation rates and functional gene abundances. Nitrification by AOA was found to play an important role in controlling N_2O emissions from tundra soil. The results improve our understanding of nitrogen transformation processes driven by microorganisms in High Arctic tundra soil.

Acknowledgments This study was funded by the National Key Research and Development Program of China (Grant no. 2020YFA0608501), the National Natural Science Foundation of China (Grant no. 41976220), and the State Key Laboratory of NBC Protection of Civilians (Grant no. SKLNBC2020-10). We acknowledge the Chinese Arctic and Antarctic Administration for support and help with the fieldwork. We thank Associate Editor Dr. Steve Coulson, Dr. Tao Bao as reviewer and another anonymous reviewer, for reviewing this manuscript.

References

Alves R, Wanek W, Zappe A, et al. 2013. Nitrification rates in Arctic soils are associated with functionally distinct populations of ammonia-oxidizing archaea. ISME J, 7(8): 1620-1631.

Baker B H, Kröger R, Brooks J P, et al. 2015. Investigation of denitrifying microbial communities within an agricultural drainage system fitted with low-grade weirs. Water Res, 87: 193-201, doi:10.1016/j.watres.2015.09.028.

Baker B J, Lesniewski R A, Dick G J. 2012. Genome-enabled transcriptomics reveals archaeal populations that drive nitrification in a deep-sea hydrothermal plume. ISME J, 6(12): 2269-2279, doi:10.1038/ismej.2012.64.

Banerjee S, Kennedy N, Richardson A, et al. 2016. Archaeal ammonia oxidizers respond to soil factors at smaller spatial scales than the overall archaeal community does in a high Arctic polar oasis. Can J Microbiol, 62: 485-491, doi:10.1139/cjm-2015-0669.

Banerjee S, Si B C, Siciliano S D. 2011. Evidence of high microbial abundance and spatial dependency in three Arctic soil ecosystems. Soil Sci Soc Am J, 75(6): 2227-2232, doi:10.2136/sssaj2011.0098.

Banerjee S, Siciliano S D. 2012a. Spatially tripartite interactions of denitrifiers in Arctic ecosystems: activities, functional groups and soil resources. Environ Microbiol, 14(9): 2601-2613, doi:10.1111/j.1462-2920.2012.02814.x.

Banerjee S, Siciliano S D. 2012b. Factors driving potential ammonia oxidation in Canadian Arctic ecosystems: does spatial scale matter? Appl Environ Microbiol, 78(2): 346-353, doi:10.1128/AEM.06132-11.

Belser L W, Schmidt E L. 1978. Diversity in the ammonia-oxidizing nitrifier population of a soil. Appl Environ Microbiol, 36(4): 584-588, doi:10.1128/aem.36.4.584-588.1978.

Bouskill N J, Eveillard D, Chien D, et al. 2012. Environmental factors determining ammonia-oxidizing organism distribution and diversity in marine environments. Environ Microbiol, 14(3): 714-729, doi:10.1111/j.1462-2920.2011.02623.x.

Bouwman L, Goldewijk K K, van der Hoek K W, et al. 2010. Correction for Bouwman et al., on May 08, 2012. Exploring global changes in nitrogen and phosphorus cycles in agriculture induced by livestock production over the 1900–2050 period. Proc Natl Acad Sci USA, 110(52): 20882-20887, 21195, doi:10.1073/pnas.1012878108.

Canion A, Overholt W A, Kostka J E, et al. 2014. Temperature response of denitrification and anaerobic ammonium oxidation rates and microbial community structure in Arctic fjord sediments. Environ Microbiol, 16(10): 3331-3344, doi:10.1111/1462-2920.12593.

Cantera J J, Stein L Y. 2007. Molecular diversity of nitrite reductase genes (*nir*K) in nitrifying bacteria. Environ Microbiol, 9(3): 765-776, doi:10.1111/j.1462-2920.2006.01198.x.

Cao H, Shockey J M, Klasson K T, et al. 2013. Developmental regulation of diacylglycerol acyltransferase family gene expression in tung tree tissues. PLoS One, 8(10): e76946, doi:10.1371/journal.pone.0076946.

Caranto J D, Lancaster K M. 2017. Nitric oxide is an obligate bacterial nitrification intermediate produced by hydroxylamine oxidoreductase. Proc Natl Acad Sci USA, 114(31): 8217-8222, doi:10.1073/pnas.1704504114.

Chen Q Q, Zhu R B, Wang Q, et al. 2014. Methane and nitrous oxide fluxes from four tundra ecotopes in Ny-Ålesund of the High Arctic. J Environ Sci, 26(7): 1403-1410, doi:10.1016/j.jes.2014.05.005.

Cheng L, Li X, Lin X, et al. 2016. Dissimilatory nitrate reduction processes in sediments of urban river networks: spatiotemporal variations and environmental implications. Environ Pollution, 219: 545-554, doi: 10.1016/j.envpol.2016.05.093.

Cowan D A, Ramond J B, Makhalanyane T P, et al. 2015. Metagenomics of extreme environments. Curr Opin Microbiol, 25: 97-102, doi:10.1016/j.mib.2015.05.005.

Daebeler A, Bodelier P L E, Hefting M M, et al. 2017. Soil warming and fertilization altered rates of nitrogen transformation processes and selected for adapted ammonia-oxidizing archaea in sub-Arctic grassland soil. Soil Biol Biochem, 107: 114-124, doi:10.1016/j.soilbio.2016.12.013.

Dai H T, Zhu R B, Sun B W, et al. 2020. Effects of sea animal activities on tundra soil denitrification and *nir*S- and *nir*K-encoding denitrifier community in maritime Antarctica. Front Microbiol, 11: 573302, doi:10.3389/fmicb.2020.573302.

Dalsgaard T, Thamdrup B, Canfield D E. 2005. Anaerobic ammonium oxidation (anammox) in the marine environment. Res Microbiol, 156(4): 457-464, doi:10.1016/j.resmic.2005.01.011.

Dalsgaard T, Thamdrup B, Farías L, et al. 2012. Anammox and denitrification in the oxygen minimum zone of the eastern South Pacific. Limnol Oceanogr, 57: 1331-1346.

Edgar R C. 2004. MUSCLE: multiple sequence alignment with high accuracy and high throughput. Nucleic Acids Res, 32(5): 1792-1797, doi:10.1093/nar/gkh340.

Fauque G, Gall J L, Barton L L. 1991. Sulfate-reducing and sulfur-reducing bacteria//Shively J M, Barton L L (Eds). Variations in autotrophic life. London: Academic Press, 271-339.

Fazzolari É, Nicolardot B, Germon J C. 1998. Simultaneous effects of increasing levels of glucose and oxygen partial pressures on denitrification and dissimilatory nitrate reduction to ammonium in repacked soil cores. Eur J Soil Biol, 34(1): 47-52, doi:10.1016/S1164-5563(99)80006-5.

Francis C A, O'Mullan G D, Cornwell J C, et al. 2013. Transitions in *nir*S-type denitrifier diversity, community composition, and biogeochemical activity along the Chesapeake Bay estuary. Front Microbiol, 4: 237, doi:10.3389/fmicb.2013.00237.

Francis C A, Roberts K J, Beman J M, et al. 2005. Ubiquity and diversity of ammonia-oxidizing archaea in water columns and sediments of the ocean. Proc Natl Acad Sci USA, 102(41): 14683-14688, doi:10.1073/pnas.0506625102.

French E, Kozlowski J A, Bollmann A. 2021. Competition between ammonia-oxidizing archaea and bacteria from freshwater environments. Appl Environ Microbiol, 87(20): e0103821, doi:10.1128/AEM.01038-21.

Galán A, Molina V, Belmar L, et al. 2012. Temporal variability and phylogenetic characterization of planktonic anammox bacteria in the coastal upwelling ecosystem off central Chile. Prog Oceanogr, 92-95: 110-120, doi: 10.1016/j.pocean.2011.07.007.

Gao D, Liu F, Li L, et al. 2018. Diversity and community structure of ammonia oxidizers in a marsh wetland of the northeast China. Appl Microbiol Biotechnol, 102(19): 8561-8571, doi:10.1007/s00253-018-9225-9.

Gao J, Hou L, Zheng Y, et al. 2016. *nir*S-Encoding denitrifier community composition, distribution, and abundance along the coastal wetlands of China. Appl Microbiol Biotechnol, 100(19): 8573-8582, doi:10.1007/s00253-016-7659-5.

Gao S, Li Z L, Hou Y A, et al. 2022. Effects of different carbon sources on the efficiency of sulfur-oxidizing denitrifying microorganisms. Environ Res, 204: 111946, doi:10.1016/j.envres.2021.111946.

Giblin A E, Nadelhoffer K J, Shaver G R, et al. 1991. Biogeochemical diversity along a riverside toposequence in Arctic Alaska. Ecol Monogr, 61(4): 415-435.

Giblin A E, Tobias C R, Song B, et al. 2013. The importance of dissimilatory nitrate reduction to ammonium (DNRA) in the nitrogen cycle of coastal ecosystems. Oceanography, 26(3): 124-131.

Hamersley M R, Lavik G, Woebken D, et al. 2007. Anaerobic ammonium oxidation in the Peruvian oxygen minimum zone. Limnol Oceanogr, 52(3): 923-933, doi:10.4319/lo.2007.52.3.0923.

Harden J W, Koven C D, Ping C L, et al. 2012. Field information links permafrost carbon to physical vulnerabilities of thawing. Geophys Res Lett, 39(15): L15704, doi: 10.1029/2012GL051958.

Hatzenpichler R. 2012. Diversity, physiology, and niche differentiation of ammonia-oxidizing archaea. Appl Environ Microbiol, 78(21): 7501-7510, doi:10.1128/AEM.01960-12.

Heylen K, Gevers D, Vanparys B, et al. 2006. The incidence of *nir*S and *nir*K and their genetic heterogeneity in cultivated denitrifiers. Environ Microbiol, 8(11): 2012-2021, doi:10.1111/j.1462-2920.2006.01081.x.

Hou L, Liu M, Carini S, et al. 2012. Transformation and fate of nitrate near the sediment-water interface of Copano Bay. Cont Shelf Res, 35: 86-94, doi:10.1016/j.csr.2012.01.004.

Hou L, Zheng Y, Liu M, et al. 2013. Anaerobic ammonium oxidation (anammox) bacterial diversity, abundance, and activity in marsh sediments of the Yangtze Estuary. J Geophys Res Biogeosci, 118(3): 1237-1246, doi:10.1002/jgrg.20108.

Hou L, Zheng Y, Liu M, et al. 2015. Anaerobic ammonium oxidation and its contribution to nitrogen removal in China's coastal wetlands. Sci Rep, 5: 15621, doi:10.1038/srep15621.

Jung M Y, Well R, Min D, et al. 2014. Isotopic signatures of N_2O produced by ammonia-oxidizing archaea from soils. ISME J, 8(5): 1115-1125, doi:10.1038/ismej.2013.205.

Kartal B, Kuypers M M M, Lavik G, et al. 2007. Anammox bacteria disguised as denitrifiers: nitrate reduction to dinitrogen gas via nitrite and ammonium. Environ Microbiol, 9(3): 635-642, doi:10.1111/j.1462-2920.2006.01183.x.

Könneke M, Bernhard A E, de la Torre J R, et al. 2005. Isolation of an autotrophic ammonia-oxidizing marine archaeon. Nature, 437(7058): 543-546, doi:10.1038/nature03911.

Kozlowski J A, Price J, Stein L Y. 2014. Revision of N_2O-producing pathways in the ammonia-oxidizing bacterium *Nitrosomonas europaea* ATCC 19718. Appl Environ Microbiol, 80(16): 4930-4935, doi:10.1128/AEM.01061-14.

Kuenen J G. 2008. Anammox bacteria: from discovery to application. Nat Rev Microbiol, 6(4): 320-326, doi:10.1038/nrmicro1857.

Kurola J, Salkinoja-Salonen M, Aarnio T, et al. 2005. Activity, diversity and population size of ammonia-oxidising bacteria in oil-contaminated landfarming soil. Fems Microbiol Lett, 250(1): 33-38, doi:10.1016/j.femsle.2005.06.057.

Kuypers M M M, Marchant H K, Kartal B. 2018. The microbial nitrogen-cycling network. Nat Rev Microbiol, 16(5): 263-276, doi:10.1038/nrmicro.2018.9.

Lam P, Jensen M M, Lavik G, et al. 2007. Linking crenarchaeal and bacterial nitrification to anammox in the Black Sea. Proc Natl Acad Sci USA, 104(17): 7104-7109.

Lam P, Lavik G, Jensen M M, et al. 2009. Revising the nitrogen cycle in the Peruvian oxygen minimum zone. Proc Natl Acad Sci USA, 106(12): 4752-4757, doi:10.1073/pnas.0812444106.

Leininger S, Urich T, Schloter M, et al. 2006. Archaea predominate among ammonia-oxidizing prokaryotes in soils. Nature, 442(7104): 806-809.

Li F, Zhu R, Bao T, et al. 2016. Sunlight stimulates methane uptake and nitrous oxide emission from the High Arctic tundra. Sci Total Environ, 572: 1150-1160, doi:10.1016/j.scitotenv.2016.08.026.

Li J, Nedwell D B, Beddow J, et al. 2015. *amo*A Gene abundances and nitrification potential rates suggest that benthic ammonia-oxidizing bacteria and not Archaea dominate N cycling in the Colne Estuary, United Kingdom. Appl Environ Microbiol, 81(1): 159-165, doi:10.1128/AEM.02654-14.

Liu K, Luo X, Jiao J J, et al. 2021. Gene abundances of AOA, AOB, and anammox controlled by groundwater chemistry of the Pearl River Delta, China. China Geol, 4(3): 463-475, doi:10.31035/cg2021054.

Lu W W, Zhang H L, Shi W M. 2013. Dissimilatory nitrate reduction to ammonium in an anaerobic agricultural soil as affected by glucose and free sulfide. Eur J Soil Biol, 58: 98-104, doi:10.1016/j.ejsobi.2013.07.003.

Ma W K, Schautz A, Fishback L A E, et al. 2007. Assessing the potential of ammonia oxidizing bacteria to produce nitrous oxide in soils of a high Arctic lowland ecosystem on Devon Island, Canada. Soil Biol Biochem, 39(8): 2001-2013, doi:10.1016/j.soilbio.2007.03.001.

Madden T. 2002. The BLAST sequence analysis tool//Beck J, Benson D, Coleman J, et al. The NCBI handbook, Bethesda (MD): National Center for Biotechnology Information (US).

Madigan M T, Martinko J M. 2006. Brock biology of microorganisms. Prentice Hall, Upper Saddle River, NJ, USA.

Marushchak M E, Pitkämäki A, Koponen H, et al. 2011. Hot spots for nitrous oxide emissions found in different types of permafrost

peatlands. Glob Change Biol, 17(8): 2601-2614.

Mosier A C, Francis C A. 2010. Denitrifier abundance and activity across the San Francisco Bay Estuary. Environ Microbiol Rep, 2(5): 667-676, doi:10.1111/j.1758-2229.2010.00156.x.

Nadelhoffer K, Giblin A, Shaver G, et al. 1992. 13 – Microbial processes and plant nutrient availability in Arctic soils. Environ Sci, 132512800, doi:10.1016/B978-0-12-168250-7.50019-5.

Nelson M B, Martiny A C, Martiny J B H. 2016. Global biogeography of microbial nitrogen-cycling traits in soil. Proc Natl Acad Sci USA, 113(29): 8033-8040, doi:10.1073/pnas.1601070113.

Nordin A, Schmidt I K, Shaver G R. 2004. Nitrogen uptake by Arctic soil microbes and plants in relation to soil nitrogen supply. Ecology, 85(4): 955-962.

Palmer K, Biasi C, Horn M A. 2012. Contrasting denitrifier communities relate to contrasting N_2O emission patterns from acidic peat soils in Arctic tundra. ISME J, 6(5): 1058-1077, doi:10.1038/ismej.2011.172.

Phillips R L, Song B, McMillan A M S, et al. 2016. Chemical formation of hybrid di-nitrogen calls fungal codenitrification into question. Sci Rep, 6: 39077, doi:10.1038/srep39077.

Qin Y, Guo J S, Fang F. 2017. Comparison on nitrosation and anaerobic ammonium oxidation between activated sludge and biofilm from an autotrophic nitrogen removal SBBR. Tecnol Cienc Agua, 8(2): 141-149, doi:10.24850/j-tyca-2017-02-13.

Rajta A, Bhatia R, Setia H, et al. 2020. Role of heterotrophic aerobic denitrifying bacteria in nitrate removal from wastewater. J Appl Microbiol, 128(5): 1261-1278, doi:10.1111/jam.14476.

Rasmussen L H, Michelsen A, Ladegaard-Pedersen P, et al. 2020. Arctic soil water chemistry in dry and wet tundra subject to snow addition, summer warming and herbivory simulation. Soil Biol Biochem, 141: 107676, doi: 10.1016/j.soilbio.2019.107676.

Rasmussen L H, Zhang W, Ambus P, et al. 2021. Correction to: Nitrogen transport in a tundra landscape: the effects of early and late growing season lateral N inputs on Arctic soil and plant N pools and N_2O fluxes. Biogeochemistry, 157(1): 85, doi:10.1007/s10533-021-00875-8.

Repo M E, Susiluoto S, Lind S E, et al. 2009. Large N_2O emissions from cryoturbated peat soil in tundra. Nat Geosci, 2(3): 189-192, doi:10.1038/ngeo434.

Rezvani F, Sarrafzadeh M H, Ebrahimi S, et al. 2019. Nitrate removal from drinking water with a focus on biological methods: a review. Environ Sci Pollut Res, 26(2): 1124-1141, doi:10.1007/s11356-017-9185-0.

Rinnan R, Michelsen A, Jonasson S. 2008. Effects of litter addition and warming on soil carbon, nutrient pools and microbial communities in a subarctic heath ecosystem. Appl Soil Ecol, 39(3): 271-281, doi:10.1016/j.apsoil.2007.12.014.

Roberts K L, Wong W W, Shimeta J, et al. 2022. Recovery of denitrification and dissimilatory nitrate reduction to ammonium following reoxygenation of sediments from a periodically hypoxic temperate lagoon. Limnol Oceanogr, 67(8): 1879-1890, doi:10.1002/lno.12173.

Rotthauwe J H, Witzel K P, Liesack W. 1997. The ammonia monooxygenase structural gene *amo*A as a functional marker: Molecular fine-scale analysis of natural ammonia-oxidizing populations. Appl Environ Microb, 63(12): 4704-4712, doi: 10.1128/aem.63.12.4704-4712.1997.

Roy D, McEvoy J, Khan E. 2020. Abundance and activity of ammonia oxidizing archaea and bacteria in bulk water and biofilm in water supply systems practicing chlorination and chloramination: full and laboratory scale investigations. Sci Total Environ, 715: 137043, doi:10.1016/j.scitotenv.2020.137043.

Rustad L, Campbell J, Marion G, et al. 2001. A meta-analysis of the response of soil respiration, net nitrogen mineralization, and aboveground plant growth to experimental ecosystem warming. Oecologia, 126(4): 543-562, doi:10.1007/s004420000544.

Rysgaard S, Glud R N, Risgaard-Petersen N, et al. 2004. Denitrification and anammox activity in Arctic marine sediments. Limnol Oceanogr, 49(5): 1493-1502, doi:10.4319/lo.2004.49.5.1493.

Salazar A, Rousk K, Jónsdóttir I S, et al. 2020. Faster nitrogen cycling and more fungal and root biomass in cold ecosystems under experimental warming: a meta-analysis. Ecology, 101(2): e02938, doi:10.1002/ecy.2938.

Salmon V G, Schadel C, Bracho R, et al. 2018. Adding depth to our understanding of nitrogen dynamics in permafrost soils. J Geophys Res Biogeo, 123(8): 2497-2512, doi: 10.1029/2018JG004518.

Santoro A E, Buchwald C, Mcilvin M R, et al. 2011. Isotopic signature of N_2O produced by marine ammonia-oxidizing archaea. Science, 333(6047): 1282-1285, doi:10.1126/science.1208239.

Schleper C. 2010. Ammonia oxidation: different niches for bacteria and archaea? ISME J, 4(9): 1092-1094, doi:10.1038/ismej.2010.111.

Shaver G, Chapin F. 1980. Response to fertilization by various plant growth forms in an Alaskan tundra: nutrient accumulation and growth. Ecology, 61: 662-675, doi:10.2307/1937432.

Siciliano S D, Ma W K, Ferguson S, et al. 2009. Nitrifier dominance of Arctic soil nitrous oxide emissions arises due to fungal competition with denitrifiers for nitrate. Soil Biol Biochem, 41(6): 1104-1110, doi:10.1016/j.soilbio.2009.02.024.

Smith J M, Mosier A C, Francis C A. 2015. Spatiotemporal relationships between the abundance, distribution, and potential activities of ammonia-oxidizing and denitrifying microorganisms in intertidal sediments. Microb Ecol, 69(1): 13-24, doi:10.1007/s00248-014-0450-1.

Spott O, Russow R, Stange C F. 2011. Formation of hybrid N_2O and hybrid N_2 due to codenitrification: first review of a barely considered process of microbially mediated N-nitrosation. Soil Biol Biochem, 43(10): 1995-2011, doi:10.1016/j.soilbio.2011.06.014.

Strous M, Fuerst J A, Kramer E, et al. 1999. Missing lithotroph identified as new planctomycete. Nature, 400(6743): 446-449, doi:10.1038/22749.

Tamura K, Dudley J, Nei M, et al. 2007. MEGA4: Molecular Evolutionary Genetics Analysis (MEGA) software version 4.0. Mol Biol Evol, 24(8): 1596-1599, doi:10.1093/molbev/msm092.

Throbäck I N, Enwall K, Jarvis Å, et al. 2004. Reassessing PCR primers targeting *nir*S, *nir*K and *nos*Z genes for community surveys of denitrifying bacteria with DGGE. Fems Microbiol Ecol, 49(3): 401-417, doi:10.1016/j.femsec.2004.04.011.

Verhamme D T, Prosser J I, Nicol G W. 2011. Ammonia concentration determines differential growth of ammonia-oxidising archaea and bacteria in soil microcosms. ISME J, 5(6): 1067-1071, doi:10.1038/ismej.2010.191.

Vipindas P V, Krishnan K P, Rehitha T V, et al. 2020. Diversity of sediment associated Planctomycetes and its related phyla with special reference to anammox bacterial community in a high Arctic fjord.

World J Microbiol Biotechnol, 36(7): 1-15, doi:10.1007/s11274-020-02886-3.

Voigt C, Marushchak M E, Lamprecht R E, et al. 2017a. Increased nitrous oxide emissions from Arctic peatlands after permafrost thaw. Proc Natl Acad Sci USA, 114(24): 6238-6243, doi:10.1073/pnas.1702902114.

Voigt C, Lamprecht R E, Marushchak M E, et al. 2017b. Warming of subarctic tundra increases emissions of all three important greenhouse gases–carbon dioxide, methane, and nitrous oxide. Glob Change Biol, 23(8): 3121-3138, doi:10.1111/gcb.13563.

Walker J K M, Egger K N, Henry G H R. 2008. Long-term experimental warming alters nitrogen-cycling communities but site factors remain the primary drivers of community structure in high arctic tundra soils. ISME J, 2(9): 982-995, doi:10.1038/ismej.2008.52.

Wang Q, Zhu R B, Zheng Y L, et al. 2019. Effects of sea animal colonization on the coupling between dynamics and activity of soil ammonia-oxidizing bacteria and archaea in maritime Antarctica. Biogeosciences, 16(20): 4113-4128, doi:10.5194/bg-16-4113-2019.

Ward B B. 2003. Significance of anaerobic ammonium oxidation in the ocean. Trends Microbiol, 11(9): 408-410, doi:10.1016/S0966-842X(03)00181-1.

Weintraub M N, Schimel J P. 2003. Interactions between carbon and nitrogen mineralization and soil organic matter chemistry in Arctic tundra soils. Ecosystems, 6(2): 129-143, doi:10.1007/s10021-002-0124-6.

Wessén E, Söderström M, Stenberg M, et al. 2011. Spatial distribution of ammonia-oxidizing bacteria and archaea across a 44-hectare farm related to ecosystem functioning. ISME J, 5(7): 1213-1225, doi:10.1038/ismej.2010.206.

Westermann S, Wollschläger U, Boike J. 2010. Monitoring of active layer dynamics at a permafrost site on Svalbard using multi-channel ground-penetrating radar. Cryosphere, 4(4): 475-487, doi:10.5194/tc-4-475-2010.

Winther J G, Godtliebsen F, Gerland S, et al. 2002. Surface albedo in Ny-Ålesund, Svalbard: variability and trends during 1981–1997. Glob Planet Change, 32(2/3): 127-139, doi:10.1016/s0921-8181(01)00103-5.

Wladyslaw P, Robert L. 2003. Aerobic and anaerobic nitrate and nitrite reduction in free-living cells of *Bradyrhizobium* sp. (*Lupinus*). FEMS Microbiol Lett, 226(2): 331-337, doi:10.1016/S0378-1097(03)00620-7.

Wuchter C, Abbas B, Coolen M J, et al. 2006. Archaeal nitrification in the ocean. Proc Natl Acad Sci USA, 103(33): 12317-12322.

Xia Y, Zhu Y G, Gu Q, et al. 2007. Does long-term fertilization treatment affect the response of soil ammonia-oxidizing bacterial communities to Zn contamination? Plant Soil, 301(1): 245-254, doi:10.1007/s11104-007-9441-z.

Yao H, Gao Y, Nicol G W, et al. 2011. Links between ammonia oxidizer community structure, abundance, and nitrification potential in acidic soils. Appl Environ Microbiol, 77(13): 4618-4625, doi:10.1128/AEM.00136-11.

Zhalnina K, de Quadros P D, Camargo F A O, et al. 2012. Drivers of archaeal ammonia-oxidizing communities in soil. Front Microbiol, 3: 210, doi:10.3389/fmicb.2012.00210.

Zhang L M, Wang M, Prosser J I, et al. 2009. Altitude ammonia-oxidizing bacteria and archaea in soils of Mount Everest. FEMS Microbiol Ecol, 70(2): 208-217, doi:10.1111/j.1574-6941.2009.00775.x.

Zhang X Z, Shen Z X, Fu G. 2015. A meta-analysis of the effects of experimental warming on soil carbon and nitrogen dynamics on the Tibetan Plateau. Appl Soil Ecol, 87: 32-38, doi:10.1016/j.apsoil.2014.11.012.

Zhao K, Kong W, Khan A, et al. 2017. Elevational diversity and distribution of ammonia-oxidizing archaea community in meadow soils on the Tibetan Plateau. Appl Microbiol Biotechnol, 101(18): 7065-7074, doi:10.1007/s00253-017-8435-x.

Zheng Y, Hou L, Liu M, et al. 2013. Diversity, abundance, and activity of ammonia-oxidizing bacteria and archaea in Chongming eastern intertidal sediments. Appl Microbiol Biotechnol, 97(18): 8351-8363, doi:10.1007/s00253-012-4512-3.

Zheng Y, Hou L, Liu M, et al. 2015. Diversity, abundance, and distribution of *nir*S-harboring denitrifiers in intertidal sediments of the Yangtze Estuary. Microb Ecol, 70(1): 30-40, doi:10.1007/s00248-015-0567-x.

Zheng Y, Wang X, Gu Y, et al. 2014. Diversity of ammonia-oxidizing archaea in Tibetan Zoige plateau wetland. Acta Microbiol Sin, 54(9): 1090-1096 (in Chinese with English abstract).

Zhu R, Chen Q , Ding W, et al. 2012. Impact of seabird activity on nitrous oxide and methane fluxes from High Arctic tundra in Svalbard, Norway. J Geophys Res, 117, G04015, doi:10.1029/2012jg002130.

Zhu R, Sun J, Liu Y, et al. 2011. Potential ammonia emissions from penguin guano, ornithogenic soils and seal colony soils in coastal Antarctica: effects of freezing-thawing cycles and selected environmental variables. Antarct Sci, 23(1): 78-92.

Supplementary Figures and Tables

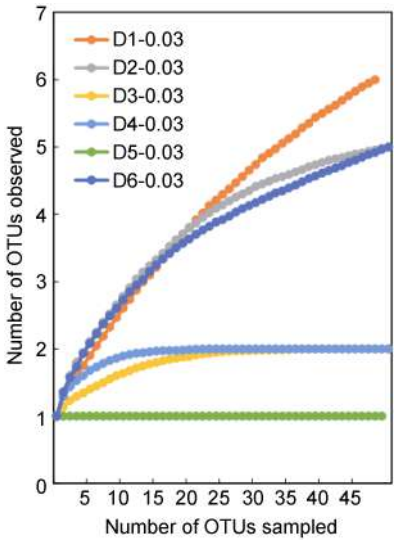

Figure S1 Rarefaction curves of the ammonia oxidizing archaeal (AOA) clone libraries. OTUs are defined at 3% divergence in nucleotides.

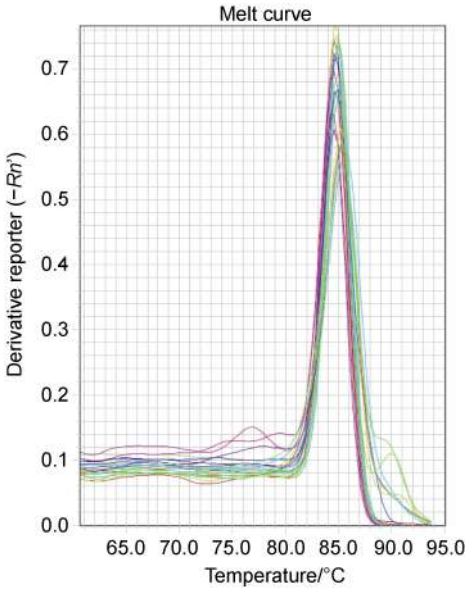

Figure S2 Melting curve of AOA *amo*A gene. Melting curve analysis had only one observable peak at a melting temperature (T_m=84.5 °C), no detectable peaks associated with primer-dimer artifacts or other non-specific PCR amplification products were observed.

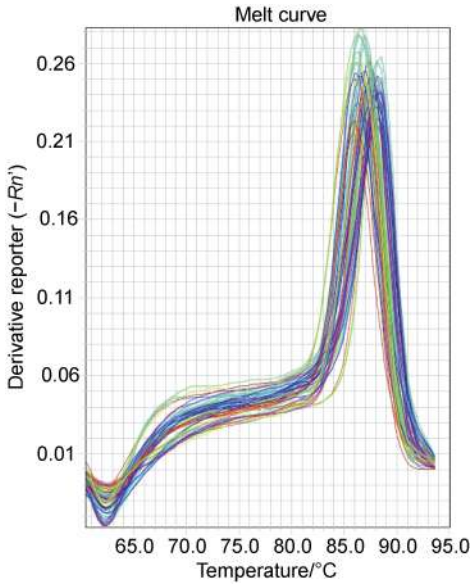

Figure S3 Melting curve of AOB *amo*A gene. Melting curve analysis had only one observable peak at a melting temperature (T_m=87.6 °C), and no detectable peaks associated with primer-dimer artifacts or other non-specific PCR amplification products were observed.

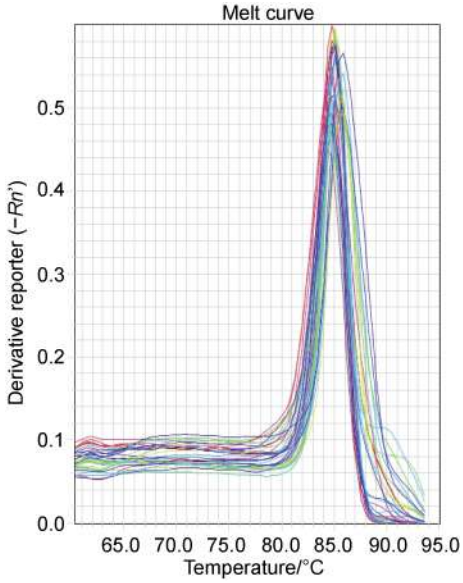

Figure S4 Melting curve of *nir*S gene. Melting curve analysis had only one observable peak at a melting temperature (T_m=84.7 °C), and no detectable peaks associated with primer-dimer artifacts or other non-specific PCR amplification products were observed.

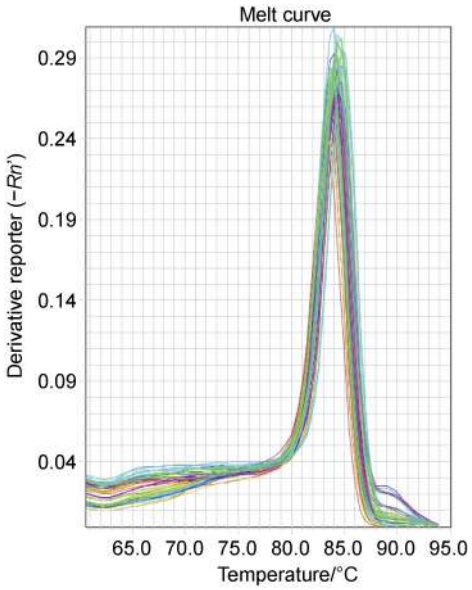

Figure S5 Melting curve of Anammox 16S rRNA. Melting curve analysis had only one observable peak at a melting temperature (T_m=84.1 °C), and no detectable peaks associated with primer-dimer artifacts or other non-specific PCR amplification products were observed.

Table S1 Primers used in the qPCR

Target gene	Primer	Primer sequence (5'-3')	References
anammox 16S rRNA	AMX-808-F	ARCYGTAAACGATGGCACTAA	Hamersley et al. (2007)
	AMX-1040-R	CAGCCATGCAACACCTGTRATA	
β-AOB *amo*A	*amo*A-1F	GGGGTTTCTACTGGTGGT	Rotthauwe et al. (1997)
	*amo*A-2R	CCCCTCKGSAAAGCCTTCTTC	
AOA *amo*A	arch-*amo*AF	STAATGGTCTGGCTTAGACG	Francis et al. (2005)
	arch-*amo*AR	GCGGCCATCCATCTGTATGT	
*nir*S	cd3aF	GTSAACGTSAAGGARACSGG	Throbäck et al. (2004)
	R3cd	GASTTCGGRTGSGTCTTGA	

Table S2 Pearson correlations (n=6) between nitrogen transformation rates and environmental variables in the soils at High Arctic tundra profile

		TC	TOC	TS	TP	TN	C:N	NH_4^+-N	NO_3^--N
Denitrification rate	*r*	0.915*	0.915*	0.605	0.381	0.874*	−0.047	0.881*	0.731
	p	0.010	0.011	0.204	0.456	0.023	0.930	0.020	0.099
Nitrification rate	*r*	0.336	0.349	0.847*	−0.689	0.358	0.122	0.143	0.490
	p	0.516	0.498	0.033	0.130	0.486	0.818	0.787	0.324
DNRA rate	*r*	0.606	0.568	0.090	0.329	0.639	−0.333	0.675	0.824*
	p	0.202	0.239	0.865	0.525	0.172	0.519	0.141	0.044

Note: * represents significant correlation

Table S3 Pearson correlations (n=6) between *nir*S, anammox 16S rRNA, AOA *amo*A, AOB *amo*A gene abundances and environmental variables in High Arctic tundra soils

		MC	TC	TOC	TS	TP	TN	C:N	NH_4^+-N	NO_3^--N
*nir*S	*r*	0.054	0.269	0.200	0.016	−0.127	0.278	−0.098	0.280	0.583
	p	0.919	0.606	0.705	0.977	0.811	0.594	0.853	0.591	0.224
anammox 16S rRNA	*r*	0.596	0.393	0.424	0.773	−0.555	0.478	−0.218	0.256	0.664
	p	0.212	0.440	0.402	0.072	0.253	0.337	0.679	0.624	0.150
AOA *amo*A	*r*	0.186	0.383	0.351	0.478	−0.500	0.414	−0.257	0.291	0.624
	p	0.724	0.453	0.495	0.337	0.313	0.415	0.623	0.575	0.186
AOB *amo*A	*r*	−0.499	−0.052	−0.105	−0.013	−0.158	−0.181	0.387	−0.114	−0.331
	p	0.314	0.922	0.843	0.981	0.765	0.732	0.449	0.830	0.522

Table S4 Pearson correlations (n=6) between *nir*S, anammox 16S rRNA, AOA *amo*A, AOB *amo*A gene abundances and nitrogen transformation rates in High Arctic tundra soils

		Denitrification rate	Nitrification rate	DNRA rate
*nir*S	*r*	−0.049	0.223	0.812*
	p	0.926	0.671	0.050
anammox 16S rRNA	*r*	0.298	0.893*	0.419
	p	0.567	0.017	0.408
AOA *amo*A	*r*	0.054	0.550	0.556
	p	0.919	0.258	0.252
AOB *amo*A	*r*	−0.042	−0.109	−0.514
	p	0.937	0.837	0.297

Note: * represents significant correlation.